JACC: BASIC TO TRANSLATIONAL SCIENCE VOL. 8, NO. 7, 2023

ORIGINAL RESEARCH - PRECLINICAL

Endothelium-Mimetic Surface Modification Improves Antithrombogenicity and Enhances Patency of Vascular Grafts in Rats and Pigs

Yongzhen Wei, PhD,[a,b,*] Huan Jiang, BS,[b,*] Chao Chai, MD,[c] Pei Liu, MS,[b] Meng Qian, PhD,[b] Na Sun, MD,[d] Man Gao, MS,[a] Honglin Zu, MD,[e] Yongquan Yu, MD,[f] Guangbo Ji, BS,[b] Yating Zhang, BS,[b] Sen Yang, MD,[e] Ju He, MD,[e] Jiansong Cheng, PhD,[a] Jinwei Tian, MD, PhD,[d] Qiang Zhao, PhD[b]

VISUAL ABSTRACT

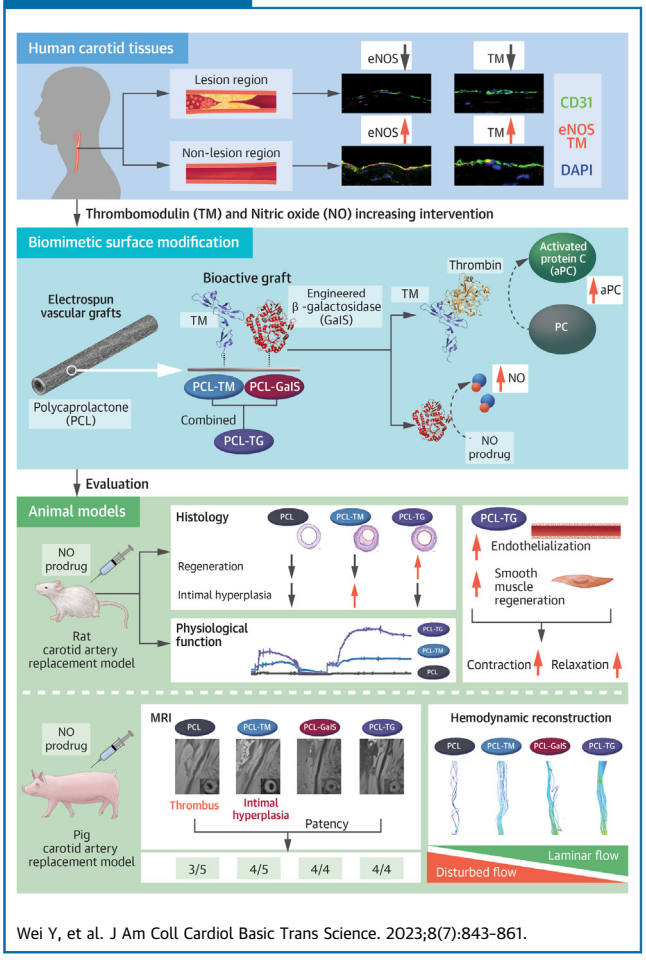

Wei Y, et al. J Am Coll Cardiol Basic Trans Science. 2023;8(7):843–861.

HIGHLIGHTS

- **TM and eNOS were identified as key factors for the antithrombogenic function of the endothelium in human atherosclerotic carotid arteries.**
- **Endothelium-mimetic surface modification of polycaprolactone vascular grafts was carried out via immobilization of recombinant TM and an engineered galactosidase responsible for the conversion of an exogenous NO prodrug.**
- **Surface modification by TM and NO cooperatively enhanced the antithrombogenicity and patency of vascular grafts in rat and pig models.**

From the [a]State Key Laboratory of Medicinal Chemical Biology, College of Pharmacy, Nankai University, Tianjin, China; [b]State Key Laboratory of Medicinal Chemical Biology, Key Laboratory of Bioactive Materials (Ministry of Education), Frontiers Science Center for Cell Responses, College of Life Sciences, Nankai University, Tianjin, China; [c]Department of Radiology, Tianjin Institute of Imaging Medicine, Tianjin First Central Hospital, School of Medicine, Nankai University, Tianjin, China; [d]Department of Cardiology,

ISSN 2452-302X https://doi.org/10.1016/j.jacbts.2022.12.009

ABBREVATIONS AND ACRONYMS

α-SMA = α-smooth muscle actin

EC = endothelial cell

eNOS = endothelial nitric oxide synthase

EPR = electron paramagnetic resonance

eSrtA = evolved *Staphylococcus aureus* sortase mutant

GalS = engineered β-galactosidase (A4-β-Gal^{H363A})

MRI = magnetic resonance imaging

NO = nitric oxide

PCL = polycaprolactone

PCNA = proliferating cell nuclear antigen

SMC = smooth muscle cell

TM = thrombomodulin

WSS = wall shear stress

SUMMARY

We first identified thrombomodulin (TM) and endothelial nitric oxide (NO) synthase as key factors for the antithrombogenic function of the endothelium in human atherosclerotic carotid arteries. Then, recombinant TM and an engineered galactosidase responsible for the conversion of an exogenous NO prodrug were immobilized on the surface of the vascular grafts. Surface modification by TM and NO cooperatively enhanced the antithrombogenicity and patency of vascular grafts. Importantly, we found that the combination of TM and NO also promoted endothelialization, whereas it reduced adverse intimal hyperplasia, which is critical for the maintenance of vascular homeostasis, as confirmed in rat and pig models. (J Am Coll Cardiol Basic Trans Science 2023;8:843–861)

Cardiovascular diseases remain a leading cause of morbidity and mortality.[1] Bypass grafting has proven successful in the treatment of cardiovascular diseases, including coronary artery disease and peripheral artery disease. Clinical practice for arterial bypass surgery continues to use autologous vascular tissue harvested from the patient as the gold standard. Nevertheless, it requires a secondary surgical site to harvest the donor graft and often has insufficient availability in patients with widespread atherosclerotic vascular disease.[2]

To address these issues, in situ tissue engineering has received increasing attention as an off-the-shelf alternative to current vascular grafts.[3-6] Upon implantation into the human body, the cell-free vascular graft will be repopulated by the host cells and gradually integrated into the autologous vascular tissue as scaffold degradation proceeds.[7-9] Unfortunately, these cell-free vascular grafts suffer from low patency due to the thrombosis in the early as well as middle/late stages before they are fully endothelialized.[10] During the last 2 decades, various types of surface modification strategies have been attempted to improve the hemocompatibility of cell-free vascular grafts.[11,12] However, outcomes after long-term implantation are far from satisfactory, and there are limited data on the translational implications in clinical trials.[13] The fundamental problem is delayed endothelial healing,[14] because a competent and functioning endothelial lining in the vascular lumen plays an important role in maintaining vascular hemostasis and patency by both secreted agents (nitric oxide [NO], prostacyclin, plasminogen) and membrane-bound species (heparan sulfate, thrombomodulin [TM]).[15]

Considering the key roles of the native endothelium, we engineered vascular grafts with an endothelium-mimicking surface to enhance graft patency and regulate vascular homeostasis. First, the key proteins involved in the pathology of atherothrombosis were identified by analyzing the human atherosclerotic carotid artery. Then, TM and engineered β-galactosidase (A4-β-Gal^{H363A}) (GalS), an enzyme for NO prodrug conversion,[16] were immobilized on the surface of vascular grafts via evolved *Staphylococcus aureus* sortase mutant (eSrtA)-mediated reversible ligation.[17] The antithrombogenic properties were evaluated by in vitro and in vivo assays, and the results indicated that TM and NO cooperatively enhanced patency and improved vascular homeostasis in both rat and pig models.

METHODS

Details of the materials and methods are available in the Supplemental Appendix. The use of experimental animals was approved by the Animal Experiments Ethical Committee of Nankai University and conducted according to the Guide for Care and Use of Laboratory Animals.

The Second Affiliated Hospital of Harbin Medical University, Key Laboratory of Myocardial Ischemia (Ministry of Education), Harbin, China; [e]Department of Vascular Surgery, Tianjin First Central Hospital, Nankai University, Tianjin, China; and the [f]Department of Radiology, Weihai Central Hospital, Weihai, China. *Drs Wei and Jiang contributed equally to this work.
The authors attest they are in compliance with human studies committees and animal welfare regulations of the authors' institutions and Food and Drug Administration guidelines, including patient consent where appropriate. For more information, visit the Author Center.

Manuscript received October 19, 2022; revised manuscript received December 29, 2022, accepted December 29, 2022.

ANALYSIS OF HUMAN ATHEROSCLEROTIC LESIONS. Fresh human carotid atherosclerotic lesion segments were obtained from donor patients who underwent carotid endarterectomy in Tianjin First Central Hospital with Institutional Review Board approval (2021N106KY). Informed consent was obtained from each patient prior to surgery. The medical information of patients is detailed in Supplemental Table 1.

STATISTICAL ANALYSIS. Statistical analysis was performed with GraphPad Prism version 9.4.1 (GraphPad Software). Continuous data are presented as the mean ± SEM, and categorical data are expressed as count and percentage. The statistical details of experiment are provided in the figure legend. The Shapiro-Wilk test was first used to assess normal distribution. For data with a normal distribution, comparisons between 2 groups were made by unpaired 2-tailed Student's *t* tests. A paired *t* test was used for assessing the difference between the lesion region and nonlesion region in the human atherosclerotic carotid artery. Comparisons among more than 2 groups were made by 1-way or 2-way analysis of variance followed by Tukey post hoc test for multiple pairwise comparisons. For data that were not normally distributed, the Kruskal-Wallis test was used for comparisons among multiple groups. Differences were considered to be significant at a P value <0.05.

RESULTS

THE EXPRESSION OF TM AND ENDOTHELIAL NO SYNTHASE IN THE ENDOTHELIUM IS REDUCED IN HUMAN ATHEROTHROMBOTIC LESIONS. Human atherosclerotic carotid artery segments were first collected and analyzed to identify the key proteins involved in the pathology of atherothrombosis (n = 10) (**Figure 1A**; patient information is presented in Supplemental Table 1). Histological staining revealed evident morphological changes, including intima hyperplasia, mineralization, and lipid accumulation in tissues containing atherosclerotic lesions compared with adjacent aorta tissues without lesions (**Figure 1B**). Consistent with previous reports,[18] we observed that the expression of KLF2 (Krüppel-like factor 2), a master regulator of shear stress-responsive genes, is reduced in endothelial cells (ECs) of human atherosclerotic lesions (**Figure 1C**). More importantly, the expression of its downstream targets, TM and endothelial nitric oxide synthase (eNOS), was also downregulated, as determined by both immunohistology (**Figure 1C**, Supplemental Figure 1A) and flow cytometry (**Figure 1D**, Supplemental Figure 1B).

Therefore, it is reasonable to speculate that deficiency of TM and eNOS mainly contributes to thrombotic lesions in patients with atherosclerosis. For this reason, surface modification of artificial vascular grafts with both NO-generating enzymes and TM is a straightforward and promising strategy to mimic the antithrombogenic function of the native endothelium, thus improving the long-term patency of the graft.

FABRICATION AND CHARACTERIZATION OF VASCULAR GRAFTS WITH ANTITHROMBOGENIC SURFACE MODIFICATION. In the present study, eSrtA was employed to reversibly immobilize bioactive molecules on the surface of vascular grafts.[19] In detail, a recombinant TM fragment containing soluble extracellular epidermal growth factor-like domains 4 through 6 and an LPETG motif (TM_{LPETG}) was expressed in *Escherichia coli* DE3. In the same way, an LPETG peptide motif was added to the C-terminus of GalS that could catalyze the decomposition of the NO prodrug MeGal-NO to release unprotected NONOates, which decompose spontaneously within several seconds to yield 2 mol of NO per mole of NONOate (Supplemental Figure 2).

In detail, vascular grafts that are surface enriched with azide were fabricated by electrospinning of polycaprolactone (PCL) doped with low-molecular-weight PCLs end-capped with azide groups.[20] As-prepared tubular grafts were first modified by alkynyl-terminated pentaglycine via click chemistry (Supplemental Figure 3). N-terminal oligoglycine nucleophiles were subsequently ligated to the LPETG motif of TM_{LPETG} and $GalS_{LPETG}$ under the catalysis of eSrtA to obtain a dual functionalized (PCL-TM and GalS [PCL-TG]) vascular graft (**Figure 2A**). The catalytic efficiency of eSrtA for peptides and proteins was measured by high-performance liquid chromatography and Western blotting, respectively (**Figure 2B**, Supplemental Figure 4).

Scanning electron microscopy images showed that electrospun vascular grafts had a well-defined fibrous structure with an average fiber diameter of 2.41 ± 0.36 μm and pore size of 11.31 ± 0.80 μm (**Figure 2C**, Supplemental Figure 5A, Supplemental Table 2). Surface modification did not alter the fiber morphology or porous architecture; however, it improved the surface hydrophilicity, as reflected by a decreased contact angle (Supplemental Figure 5B). The mechanical properties of the vascular grafts before and after surface modification were compared by tensile testing, and no evident changes were detected (Supplemental Table 3, Supplemental Figure 5C).

FIGURE 1 The Expression of TM and eNOS in the Endothelium Is Reduced in Human Atherothrombotic Lesions

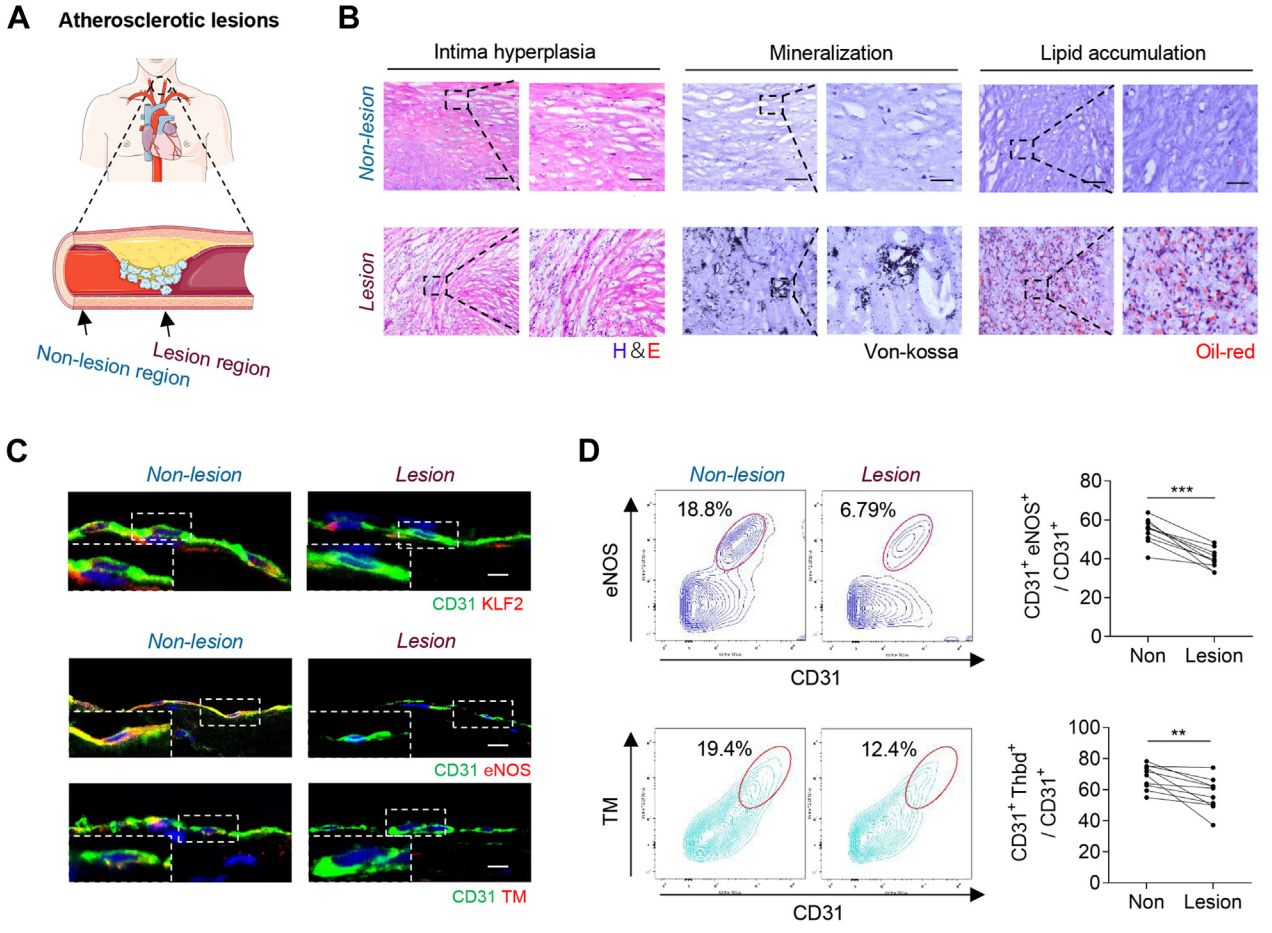

(A) Schematic illustration of the carotid artery from atherosclerotic patients. **(B)** Representative hematoxylin and eosin (H&E), Von Kossa, and Oil red O staining images of human carotid artery segments with and without atherosclerotic lesion (n = 10). Scale bars = 100 μm **(left)**, 50 μm **(right)**. **(C)** The arterial endothelium was further analyzed by immunofluorescence staining for CD31 **(green)** and KLF2 **(red)**, eNOS **(red)**, and thrombomodulin **(red)**, respectively (n = 10). Nuclei were stained with DAPI **(blue)**. Scale bar = 10 μm. **(D)** Representative images of flow cytometry assay and quantification of the percentage of endothelial nitric oxide synthase (eNOS)-positive and thrombomodulin (TM)-positive cells within the $CD31^+$ cells (n = 10). Statistical significance was assessed by paired Student's *t* test. Data are expressed as mean ± SEM. $^{**}P < 0.01$ and $^{***}P < 0.001$. KLF2 = Krüppel-like factor 2.

The bioactivity of the functional molecules (TM and A4-β-Gal^{H363A}) immobilized on the vascular grafts was further assessed. Immobilized TM was responsible for anticoagulant activity via the alteration of thrombin substrate specificity (**Figure 2D**). The results showed that PCL-TG vascular grafts could catalyze activated protein C generation in a solution of protein C and thrombin (**Figure 2D**), and the TM immobilized on the PCL-TG was quantified with a density value of 0.72 ± 0.06 μg/mm^2 (Supplemental Figure 6). To evaluate the catalytic activity of immobilized GalS for the conversion of the NO prodrug, NO release behavior was evaluated using a Griess assay. PCL-GalS and PCL-TG vascular grafts exhibited catalytic activity that was similar to that of free GalS at a concentration of 0.01 mg/mL (**Figure 2E**) and the density of GalS immobilized on the PCL-TG was 0.12 ± 0.02 μg/mm^2 (Supplemental Figure 6).

PRECISE AND TARGETED DELIVERY OF NO TO VASCULAR GRAFTS IN VIVO. In vivo NO release catalyzed by enzymes immobilized on the vascular grafts was evaluated in a rat carotid artery replacement model. The prodrug MeGal-NO was administered via tail vein injection, and when it reached the site of the functionalized vascular graft, immobilized

FIGURE 2 Fabrication and Characterization of Antithrombogenic Modified Vascular Grafts

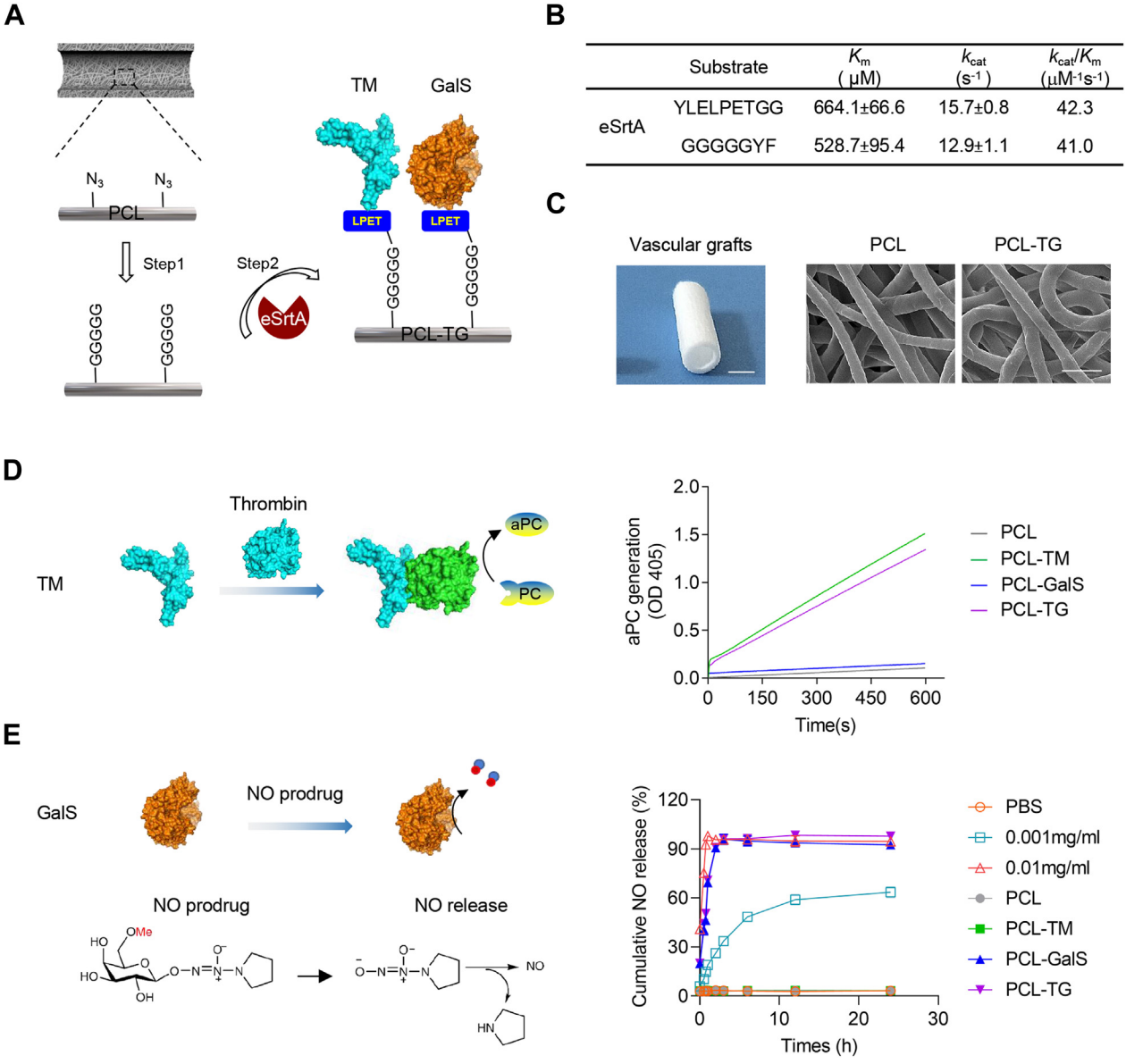

	Substrate	K_m (μM)	k_{cat} (s^{-1})	k_{cat}/K_m ($\mu M^{-1}s^{-1}$)
eSrtA	YLELPETGG	664.1±66.6	15.7±0.8	42.3
	GGGGGYF	528.7±95.4	12.9±1.1	41.0

(A) Fabrication of antithrombogenic modified vascular grafts via surface immobilization of thrombomodulin (TM) and engineered β-galactosidase (A4-β-Gal^{H363A}) (GalS) catalyzed by evolved *Staphylococcus aureus* sortase mutant (eSrtA). **(B)** Apparent kinetic parameters of eSrtA. Data are expressed as mean ± SEM. (n = 3). **(C)** Representative image of the electrospun vascular graft (scale bar = 2 mm) as well as the microstructure observed by scanning electron microscopy (scale bar = 20 μm) before and after modification. **(D)** Schematic illustration of activated protein C (aPC) generation from the TM immobilized surface. The production of aPC from vascular grafts was detected using an enzymatically digestible chromogenic assay. **(E)** Schematic illustration depicting the conversion of nitric oxide (NO) prodrug (MeGal-NO) into NO under the catalysis of surface-immobilized GalS. Releasing curves illustrating the generation of NO from the NO prodrug (0.03 mg/mL) by the vascular grafts. Free GalS at different concentrations (0, 0.001, 0.01 mg/mL) was used as a control. Data are expressed as mean ± SEM. n = 3. PBS = phosphate-buffered saline; PC = protein C; PCL = polycaprolactone.

GalS could catalyze the conversion of MeGal-NO into NO (Figure 3A). Local NO generation by the implanted vascular grafts was evaluated using an electron paramagnetic resonance (EPR) assay using Fe-DETC as the spin-trapping reagent (Figure 3B). A stronger triplet with a central g value of 2.041 and hyperfine splitting of 12.78 G $(DETC)_2$Fe-NO adduct was observed on the EPR spectrum of the extracts from

FIGURE 3 In Vivo Catalytic Property and Rechargeability of the Enzymes Immobilized on the Surface of Functionalized Vascular Grafts

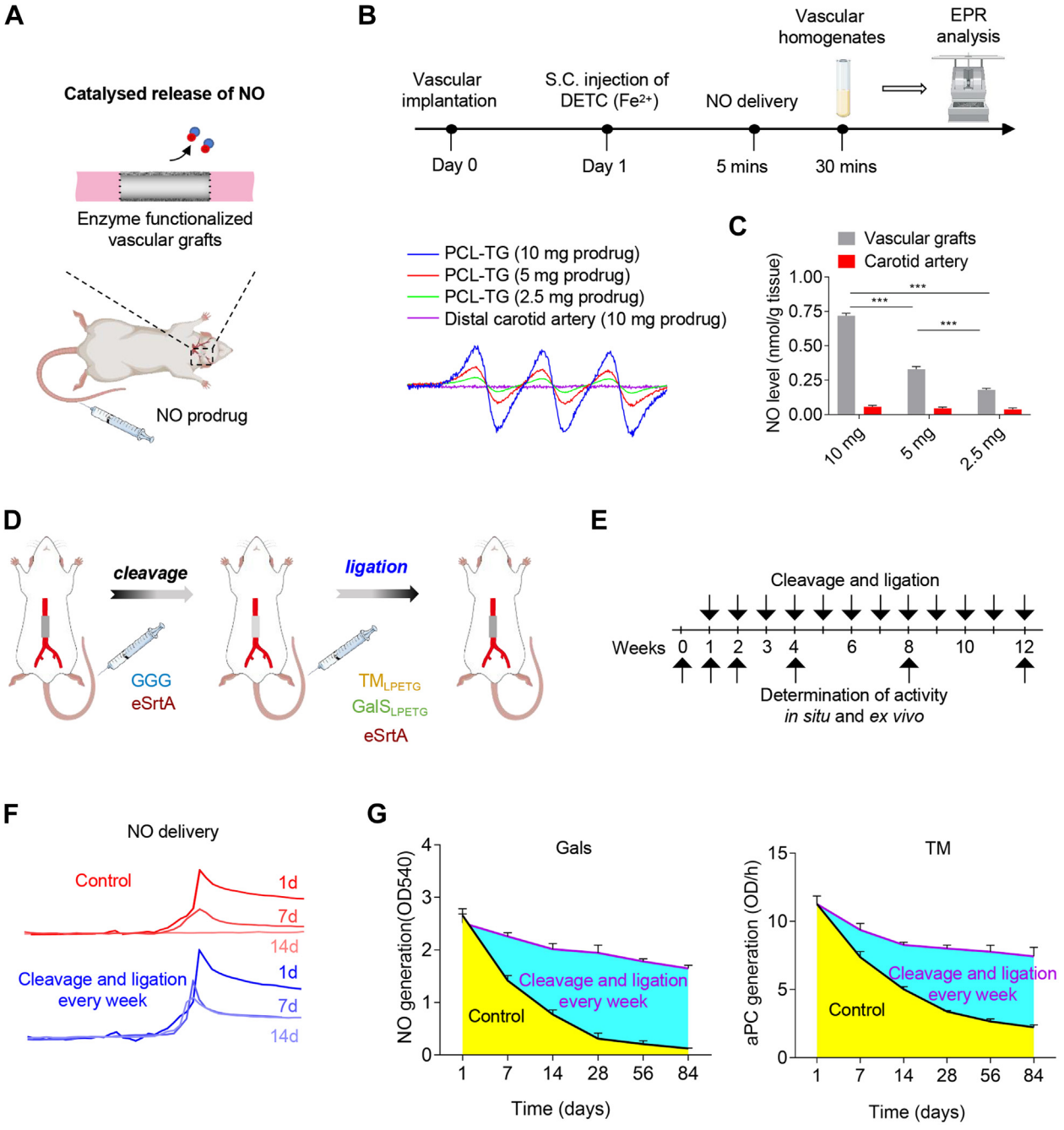

(A) Schematic Illustration representing the in situ conversion of NO prodrug into NO under the catalysis of GalS immobilized on the surface of vascular grafts. **(B)** Representative electron paramagnetic resonance (EPR) spectra reflecting NO generation within the vascular grafts in the presence of (DETC)2Fe. **(C)** NO levels in the native artery and vascular grafts were determined by the quantitation of (DETC)2Fe-NO complex using TEMPO (n = 3). **(D, E)** Schematic illustration and experimental schedule for the detection of in vivo rechargeability of enzymes immobilized on the graft surface in a rat abdominal aorta replacement model. **(F)** In situ NO releasing property of functionalized vascular grafts was monitored using an NO-sensitive electrode. **(G)** The activities of GalS and TM on the functionalized vascular grafts were further analyzed after explantation (n = 3-4). Statistical significance was assessed by 1-way analysis of variance followed by Tukey's post hoc analysis. Data are expressed as mean ± SEM. ***$P < 0.001$. S.C. = subcutaneous; other abbreviations as in Figure 2.

PCL-TG vascular grafts than those from control PCL vascular grafts. Further quantitative analysis showed that the NO level in the vascular grafts was closely related to the concentration of the prodrug, whereas those in native blood vessels (the carotid artery next to the distal end of implanted vascular grafts) did not show detectable difference among 3 groups (**Figure 3C**). Because the terminal elimination half-life (t1/2) for MeGal-NO was 1.2 hours,[16] NO generation from the vascular grafts is not continuous, and a higher level of NO generation could be obtained during the first couple of hours after drug administration. All these results indicate that PCL-TG vascular grafts allow the precise and controlled delivery of NO and that local generation of exogenous NO from vascular grafts cannot alter the systemic NO level to induce adverse effects.

RECHARGEABILITY OF ENZYMES IMMOBILIZED ON THE SURFACE OF VASCULAR GRAFTS. The reversible immobilization of bioactive molecules on the oligoglycine-modified surfaces of vascular grafts was evaluated (Supplemental Figure 7A), and the results indicated that repeated cleavage and ligation of GalS and TM could be achieved by eSrtA. Notably, the bioactivity of GalS and TM on the vascular grafts remained unchanged after 3 cycles of cleavage and ligation (Supplemental Figure 7B). To visualize the distribution of immobilized TM or GalS, we further performed His staining for PCL-TM and PCL-GalS grafts. Uniform distribution of TM or GalS was observed on the graft surface. The signal of immobilized motifs (GalS or TM) remained unchanged even after several cycles of cleavage and ligation (Supplemental Figure 7C).

In vivo rechargeability was further evaluated 12 weeks after the implantation of vascular grafts into the infrarenal abdominal aortas of rats (**Figures 3D and 3E**). The efficiency of cleavage and ligation steps was evaluated by using a fluorescence probe, MeGal-DDAO (Supplemental Figure 8). Results showed that the cleavage and ligation of GalS and TM can also be achieved after 12 weeks of implantation. In situ NO generation from the vascular grafts implanted in the rats was assessed with an NO-sensitive electrode. In the control group, the NO signal decreased rapidly within 1 week and almost disappeared by 2 weeks after implantation. In contrast, the de novo functionalized surface retained a high level of catalytic activity; that is, the signal was >50% after 2 weeks (**Figure 3F**). Then, the vascular grafts were explanted at the indicated time points, and the bioactivity of GalS and TM immobilized on the vascular grafts was measured (**Figure 3G**). The results demonstrated that the bioactivity of both GalS and TM remained relatively high for up to 3 months due to cyclic cleavage and ligation, whereas the bioactivity of the control grafts decreased consistently with time.

It is worth noting that the residual enzyme activity of GalS was higher than that observed in situ. This is because the prodrug circulated and only contacted the inner surface of the vascular graft in the in situ assay, while the explanted graft was fully immersed in the prodrug solution in the ex vivo assay; hence, more enzyme was available within the graft wall to catalyze NO release.

TM AND NO COOPERATIVELY ENHANCE SURFACE HEMOCOMPATIBILITY OF VASCULAR GRAFTS. In vivo hemocompatibility of the vascular grafts was first evaluated in rat carotid artery replacement models. Three days after implantation, all the grafts were collected, and the acute thrombotic response on the grafts was evaluated (**Figure 4A**). Hematoxylin and eosin and periodic acid-Schiff staining showed that the surfaces of the dual functionalized (PCL-TG) vascular grafts were clean compared with those of the other graft types, in which acute fibrin thrombi had formed (**Figure 4B**). Fibrinogen deposition on the vascular grafts was further tested by enzyme-linked immunosorbent assay (**Figure 4C**). Platelet-leukocyte aggregation, an integral process underlying the interaction between platelets and leukocytes, is recognized as a key contributor to thrombosis. Scanning electron microscopy images also showed that surface modification by TM and GalS markedly reduced platelet-leukocyte aggregation, with PCL-TG vascular grafts being the most effective (**Figures 4D and 4E**).

Generally, the formation of thrombi is closely related to thrombin activation and platelet aggregation. Hence, the effect of TM and NO on thrombin activation was investigated using a known protein solution containing fibrinogen. As shown in **Figure 4F**, the absorption exhibited an initial rise followed by a plateau. The initial rate and final optical density are shown in Supplemental Table 4. The polymerization of fibrinogen was markedly inhibited by TM but moderately inhibited by NO, suggesting that TM is more capable of neutralizing thrombin than NO. The inhibitory effect was more pronounced in the group treated with TM and NO, indicating that they exerted a cooperative effect. A platelet aggregation assay showed that collagen-induced aggregation of human platelets was evidently delayed after NO treatment, and this delay could be further synergistically enhanced by TM (**Figure 4G**). In contrast, TM alone had a lower capacity to inhibit platelet aggregation

FIGURE 4 TM and NO Cooperatively Enhance Surface Hemocompatibility of Vascular Grafts In Vivo and In Vitro

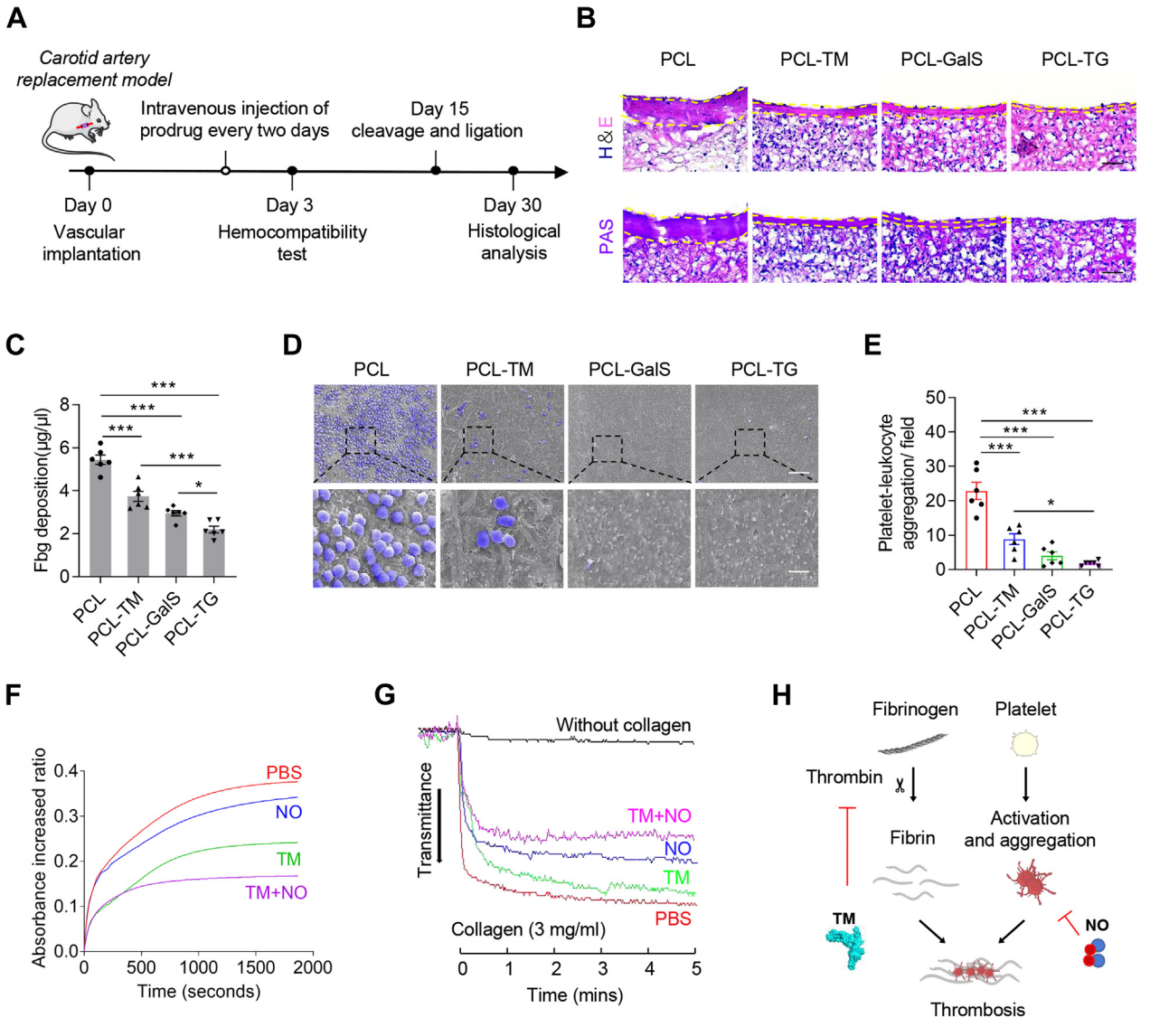

(A) Experimental design for evaluation of the vascular grafts in a rat carotid artery replacement model. **(B)** H&E **(top)** and periodic acid-Schiff (PAS) **(bottom)** staining on cross-sections of vascular grafts (PCL, PCL-TM, PCL-GalS, and PCL-TG) at 3 days postimplantation. The **yellow dotted line** indicates the adhesive proteins on the graft wall. Scale bar = 100 μm. **(C)** Adsorption of plasma fibrinogen on the vascular grafts was measured by enzyme-linked immunosorbent assay (n = 6). **(D)** Platelet-leukocyte aggregation (PLA) on the luminal surface of explanted vascular grafts was observed by scanning electron microscopy. Leukocytes were false-colored with **purple**. Scale bars = 100 μm **(top)**, 10 μm **(bottom)**. **(E)** The quantification of PLA based on scanning electron microscopy images (n = 6). **(F)** Fibrin polymerization curves show the response of thrombin activity after treatments with NO (100 μM), TM (10 μM), or TM combined with NO, respectively. **(G)** Human platelets of equal quantity were incubated with NO (100 μM), TM (10 μM), or TM combined with NO, respectively. Aggregation profile was determined in the presence of thrombin (3 mg/mL at initiated points indicated by **arrows**). **(H)** Schematic illustration of the synergistic effect of TM and NO on antithrombosis. Statistical significance was assessed by 1-way analysis of variance followed by Tukey's post hoc analysis. Data are expressed as mean ± SEM. *$P < 0.05$ and ***$P < 0.001$. Fbg = fibrinogen; other abbreviations as in Figures 1 and 2.

than NO. All these results showed that TM and NO effectively reduce thrombosis via cooperative mechanisms (Figure 4H). The results were in line with those of the in vivo assay.

The hemocompatibility of vascular grafts was further evaluated by an ex vivo arteriovenous shunt assay in hyperlipidemic rats (Supplemental Figure 9A) in order to mimic the vessel grafting in

patients with chronic disease in clinical setting.[21] Interestingly, less thrombus formation was observed in the dual functionalized vascular grafts (PCL-TG) than in the other 2 graft types (PCL-TM and PCL-GalS vascular grafts) (Supplemental Figures 9B and 9C). TM suppressed platelet adhesion to some degree, and more pronounced inhibition was observed in the PCL-GalS and PCL-TG groups due to NO supplementation (Supplemental Figure 9D). In brief, both platelet adhesion and platelet activation were significantly reduced in the PCL-TG group compared with the other 3 groups (Supplemental Figures 9E and F).

ANTITHROMBOGENIC SURFACE MODIFICATION ENHANCES ENDOTHELIALIZATION AND REDUCES INTIMAL HYPERPLASIA IN RATS. Tissue regeneration in vascular grafts were further evaluated in a rat model of carotid artery replacements after 1 month implantation. Histological analysis (**Figures 5A and 5B**) revealed severe luminal narrowing in the PCL-TM group due to intimal hyperplasia. In contrast, exogenous NO supplementation effectively inhibited the adverse intimal remodeling. Instead, a well-defined layer of neointima with proper thickness was seen on the luminal surface of the PCL-TG grafts.

Endothelial coverage on the luminal surface was first observed by scanning electron microscopy. Compared with the other 3 graft types, PCL-TG grafts demonstrated rapid endothelialization at 1 month; the lumen was almost completely covered with cobblestone-like ECs, and very few bare fibers could be identified in the middle portion of the graft (Supplemental Figure 10). Immunofluorescence staining showed that luminal coverage of $CD144^+$ and $CD31^+$ cells was both significantly higher in the PCL-TG group than in the other 3 groups at 1 month (**Figures 5C and 5D**, Supplemental Figure 11). The results were further supported by en face staining for CD31 and CD144 (**Figure 5E**). Vascular smooth muscle regeneration was assessed by costaining for α-smooth muscle actin (α-SMA) and MYH11, which are markers of contractile proteins. The PCL-TG group showed enhanced smooth muscle regeneration at 1 month, as characterized by a well-organized layer of $\alpha\text{-SMA}^+$ $MYH11^+$ smooth muscle cells (SMCs) that were circumferentially aligned in a fashion similar to the media of the native artery. Furthermore, the number of $\alpha\text{-SMA}^+$ $MYH11^+$ cells was markedly enhanced in the PCL-TG group compared with other groups (**Figure 5F**). In contrast, fewer double-positive cells could be identified in the PCL-TM group despite the increased number of $\alpha\text{-SMA}^+$ cells, indicating that most of these SMCs maintained proliferative phenotype. Flow cytometry assay revealed that TM alone decreased the percentage of $\alpha\text{-SMA}^+$ $CNN1^+$ cells relative to total cells digested from explanted vascular grafts at 1 month (Supplemental Figure 12).

Flow cytometry assay was also performed to identify proliferative cells from ECs ($CD31^+$) and SMCs ($\alpha\text{-SMA}^+$) by combined with proliferating cell nuclear antigen (PCNA) staining (**Figure 5G**). TM modification significantly increased the proliferation of vascular cells, that is, the percentage of $CD31^+PCNA^+$ and $\alpha\text{-SMA}^+$ $PCNA^+$ cells were both increased compared with the control PCL group due to the mitogenic activity of TM. Therefore, it is an important factor contributing to the endothelialization, whereas overproliferation of SMCs leads to the intimal hyperplasia in the PCL-TM graft. This is in line with previous studies showing that local overexpression of TM can prevent early vein graft failure by inhibiting thrombosis but fails to reduce late failure generally caused by intimal hyperplasia.[22]

On the other hand, the influence of NO on EC proliferation is dose dependent; within an appropriate dosage range, exogenous NO also promoted EC proliferation and exhibited a synergistic effect with TM, as evidenced by in vitro experiments (Supplemental Figure 13). In the case of high dosage, EC proliferation was evidently inhibited due to the toxicity of NO, while TM provided a protective effect against cell death.

The cooperative effect of TM and NO on endothelialization has also been supported by in vitro assays, including cell adhesion, migration, and tube formation of ECs (Supplemental Figure 14). To further elucidate the underlying mechanism, we investigated the activation of ERK and AKT pathway in ECs, which have been shown to be involved in the proliferation and migration of ECs.[23-25] The phosphorylation of ERK and AKT were assessed by Western blotting after 0 to 60 minutes of NO or TM stimulation (Supplemental Figures 15A and 15B). Both NO and TM can activate ERK and AKT signaling, whereas treatment with ERK inhibitor (PD98059) and AKT inhibitor (LY294002) inhibited cell migration and proliferation induced by TM or NO stimulation (Supplemental Figures 15C and 15D), indicating that ERK and AKT signaling pathways were required for EC proliferation and migration induced by TM or NO.

As an important signaling molecule, NO also demonstrated a regulatory effect on SMC differentiation; it could promote the transition of SMCs into a contractile phenotype that showing low proliferation capability at both high and low dosage (Supplemental Figure 16). Despite the contradictory roles that TM and NO played on the SMC proliferation, combination of them also exhibited an inhibitory effect; thus,

FIGURE 5 **Antithrombogenic Surface Modification Promotes Endothelialization and Reduces Intimal Hyperplasia of Vascular Grafts in a Rat Model**

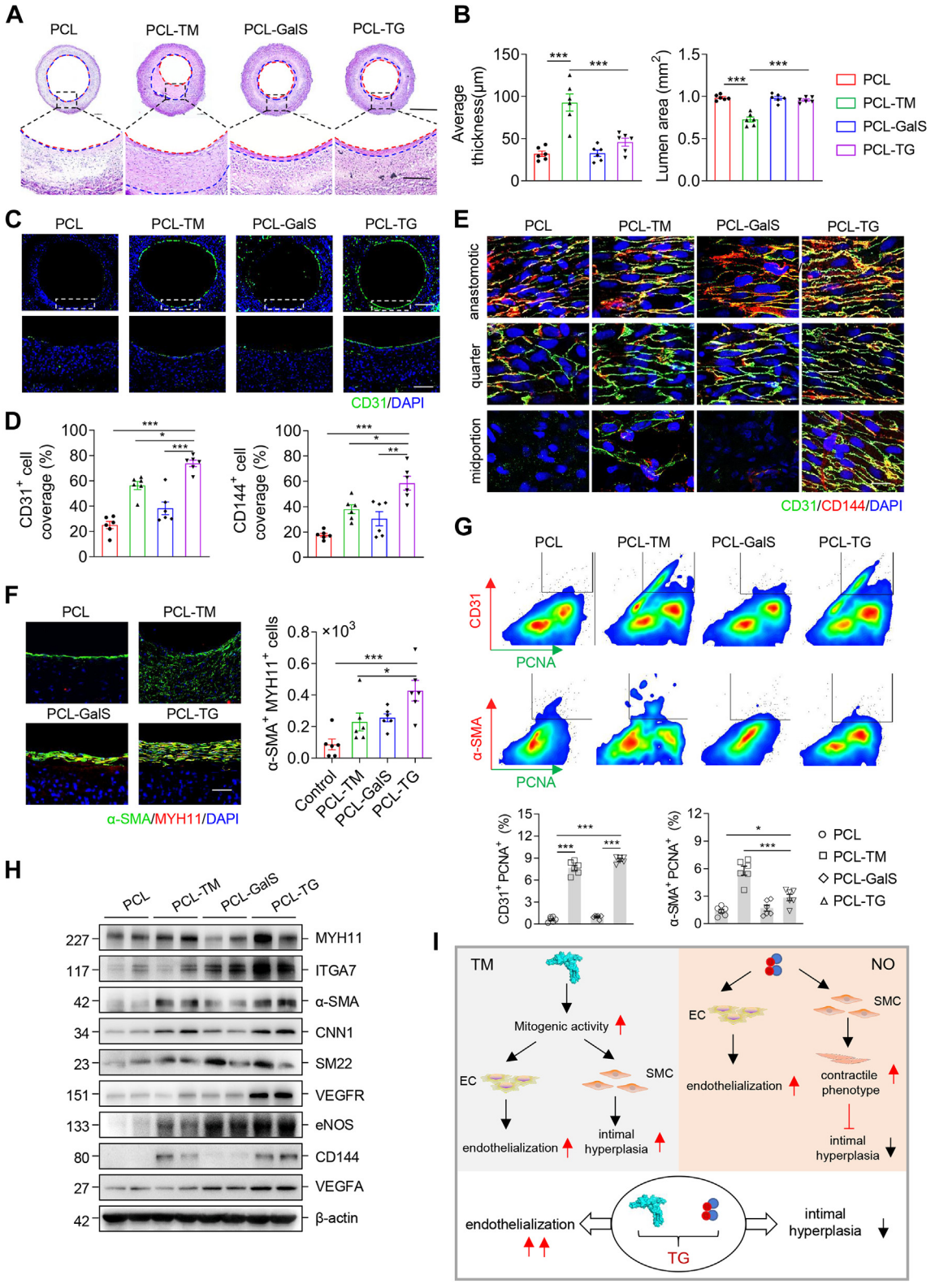

Continued on the next page

reduced intimal hyperplasia was observed in the PCL-TG grafts accordingly.

The expression levels of proteins related to SMCs (MYH11, ITGA7, α-SMA, CNN1, and SM22) and ECs (vascular endothelial growth factor receptor, eNOS, CD144, and vascular endothelial growth factor A) were analyzed by Western blotting (Figure 5H). All these results indicate that TM and NO cooperatively promoted endothelialization, whereas it reduced adverse intimal hyperplasia, which is critical for the maintenance of vascular homeostasis, unlike the surfaces modified by TM or NO alone (PCL-TM and PCL-GalS) (Figure 5I).

ANTITHROMBOGENIC FUNCTIONALIZED SURFACES INDUCE FUNCTIONAL TISSUE REGENERATION AFTER LONG-TERM IMPLANTATION. Long-term implantation in rats further demonstrated that tubular morphology of the grafts has been well maintained and no stenosis or dilation occurred at 3 months. Importantly, the average thickness of neotissue was markedly higher in the PCL-TG group than in other groups (Figures 6A and 6B). Endothelialization was evaluated by immunofluorescence staining with CD144 and eNOS antibodies (Figure 6C). TM and NO cooperatively enhanced competent and functional endothelial regeneration with highest luminal coverage of $CD144^+eNOS^+$ cells obtained in the PCL-TG group. Vascular smooth muscle maturation was assessed by costaining for CNN1 and MHC (major histocompatibility complex), which are markers of contractile proteins. Compared with the other groups, the PCL-TG group showed enhanced regeneration of contractile smooth muscle at 3 months, as characterized by a well-organized layer of $CNN1^+$ MHC^+ SMCs that were circumferentially aligned in a fashion similar to the media of the native artery (Figure 6D).

The physiological vasomotor function of vascular grafts explanted at 3 months was tested by standard dual-wire myography (Figure 6E). Compared with the other groups, the PCL-TG group showed significantly enhanced vasoconstriction in response to KCl and adrenaline. The contraction could be subsequently inhibited by vasodilation after acetylcholine treatment. All these results indicate that the regenerated vascular tissue holds potent vasomotor function.

The effect of surface modification on the chronic inflammatory response after long-term implantation was also investigated. Infiltration of T cells and macrophages within the vascular grafts post-implantation was detected by using CD3 and CD68 antibodies, respectively. Results showed that surface modification did not affect the infiltration of T cells or macrophages (Supplemental Figure 17). In addition, TM and NO alone or in combination could effectively promote the polarization of macrophages towards a protective anti-inflammatory (M2) phenotype, as evidenced by the reduced density of $iNOS^+$ M1 macrophages and increased density of $CD206^+$ M2 macrophages in the modified vascular grafts (PCL-TM, PCL-GalS, PCL-TG). It was further confirmed by the expression of proinflammatory cytokines (interleukin-1β and tumor necrosis factor α) (Supplemental Figure 18).[26-28]

ANTITHROMBOGENIC SURFACE MODIFICATION ENHANCES PATENCY AND IMPROVE HEMODYNAMIC PERFORMANCE OF VASCULAR GRAFTS IN PIGS. The patency and healing performance of functionalized vascular grafts were further evaluated in a preclinical large animal model (Figure 7A). Clinically relevant-sized vascular grafts (3.8 mm in diameter and 4 cm in length) were implanted into the bilateral carotid arteries of pigs in an end-to-end fashion (Figure 7B). Blood circulation was re-established, and continuous turbulent flow was detected by color Doppler ultrasonography immediately after anastomosis (Figure 7B).

The patency of the implanted grafts was first monitored by computed tomography and

FIGURE 5 Continued

(A) H&E staining of vascular grafts explanted at 1 month. Scale bars = 1 mm **(top)**, 100 μm **(bottom)**. **(B)** Quantification of the neointima thickness and lumen area based on H&E staining (n = 6). **(C)** Immunofluorescence staining of cross-sections by CD31 **(green)**. Scale bars = 1 mm **(top)**, 100 μm **(bottom)**. **(D)** The regeneration of endothelium was further quantified by determining the coverage of $CD144^+$ cells and $CD31^+$ cells on the luminal surface at different sites (suture, quarter, and middle) (n = 6). **(E)** En face staining of CD31 **(green)** and CD144 **(red)** showing enhanced endothelialization in PCL-TG vascular grafts compared with other groups at 1 month. Scale bar = 20 μm. **(F)** Immunofluorescence staining by α-smooth muscle actin (α-SMA) **(green)** and MYH11 **(red)**. Scale bar = 100 μm. The number of $\alpha\text{-SMA}^+MYH11^+$ cells within the neotissue was further quantified (n = 6). **(G)** Representative images of flow cytometry assay and quantification of the percentage of $CD31^+$ proliferating cell nuclear antigen (PCNA)–positive and $\alpha\text{-SMA}^+$ $PCNA^+$ cells in total cells digested from explanted vascular grafts (n = 6). **(H)** Representative Western blot showed expression levels of smooth muscle cell (SMC)– and endothelial cell (EC)–related proteins in explanted vascular grafts. **(I)** Mechanistic summary of the synergistic effect of TM and NO on vascular regeneration and remodeling. Statistical significance was assessed by 1-way analysis of variance followed by Tukey's post hoc analysis **(B, D, G)** or Kruskal-Wallis test with Dunn's multiple comparisons **(F)**. Data are expressed as mean ± SEM. $*P < 0.05$, $**P < 0.01$, and $***P < 0.001$. VEGFA = vascular endothelial growth factor A; VEGFR = vascular endothelial growth factor receptor; other abbreviations as in Figures 1 and 2.

FIGURE 6 Antithrombogenic Surface Modification Induces Functional Tissue Regeneration After Long-Term Implantation in a Rat Model

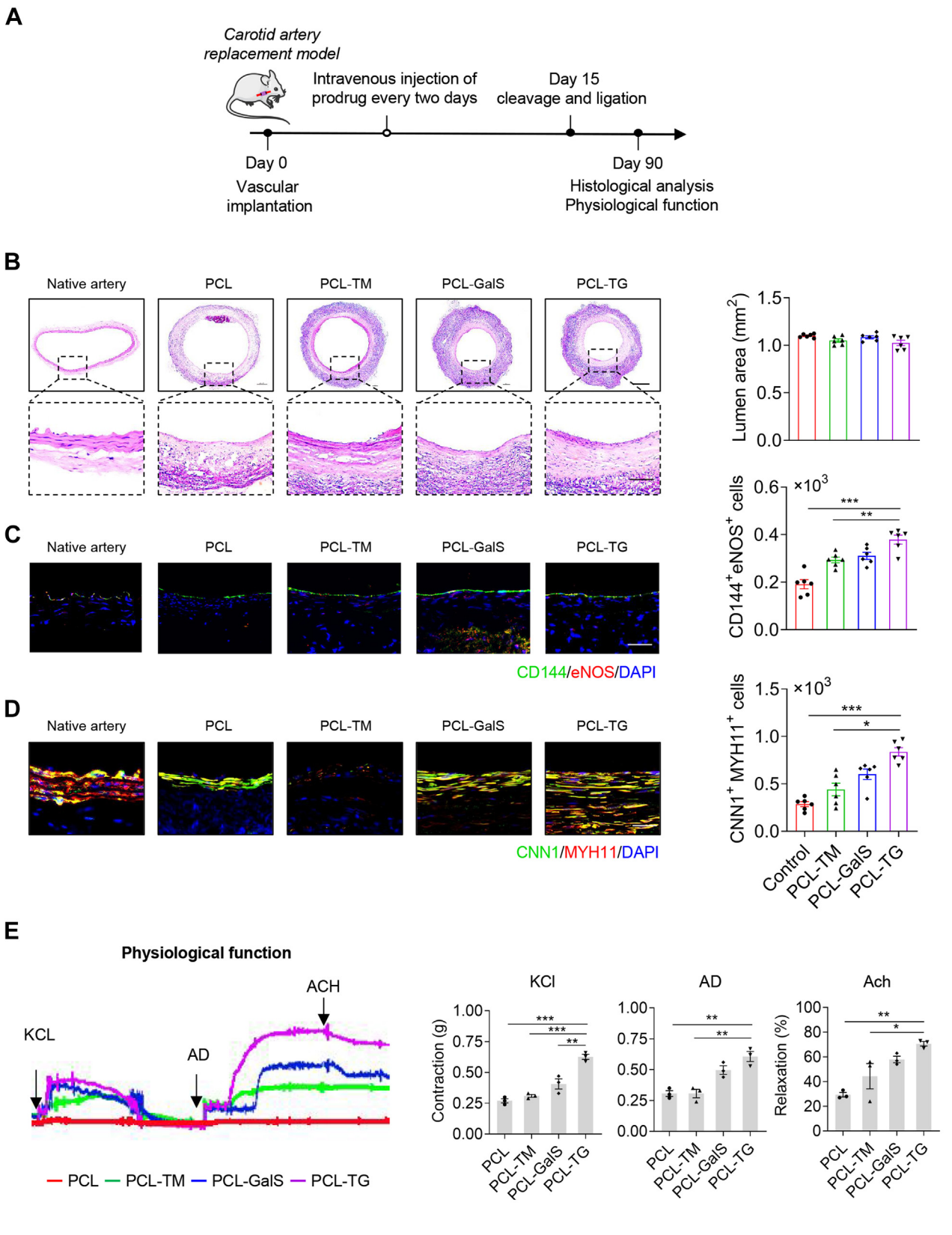

Continued on the next page

ultrasonography (**Figure 7C**, Supplemental Figure 19) at different time points (weeks 1, 2, and 4). In general, PCL-GalS and PCL-TG vascular grafts (4/4 and 4/4) showed higher levels of patency than PCL and PCL-TM vascular grafts (3/5, 3/4) (**Figure 7D**).

The reason for the occlusion in the PCL and PCL-TM groups was also analyzed by magnetic resonance imaging (MRI). Images from occluded PCL grafts showed hyperintensity in T1 and hypointensity in T2, indicating the formation of thrombi. In contrast, a specific signal consisting of 2 distinct layers appeared in the occluded PCL-TM grafts. The outer layer, which was in direct contact with the luminal surface, demonstrated hypointensity in T1 and hyperintensity in T2, indicating intimal hyperplasia. The other layer exhibited hyperintensity in T1 and hypointensity in T2, indicating thrombosis (Supplemental Figure 20A). It is reasonable to deduce that TM first induces intimal hyperplasia, consequently leading to hemodynamic changes and thrombus formation. Histological analysis of the explanted vascular grafts at 1 month further confirmed these findings (Supplemental Figure 20B). The lumens of the occluded PCL grafts were entirely filled with thrombi. In contrast, a thick neointimal layer rich in α-SMA^{+} cells was observed between the thrombus and graft wall in the PCL-TM group (Supplemental Figure 20C).

The patent vascular grafts were further investigated by MRI (**Figure 7E**). Although some grafts in the PCL and PCL-TM groups remained patent, the lumens of the grafts were also occupied by mural thrombi (hyperintensity in T1 and hypointensity in T2, indicated by the red arrowhead) and intimal hyperplasia (hypointensity in T1 and hyperintensity in T2, indicated by the yellow arrow) to a certain degree. However, both the formation of mural thrombi and intimal hyperplasia were evidently inhibited in the PCL-GalS and PCL-TG groups due to supplementation with the NO prodrug. It is worth mentioning that a signal with hyperintensity in T1 and hyperintensity in T2, which was attributed to the normal vascular regeneration (indicated by the green arrow), was detected on the luminal surface of the PCL-TG grafts.

Blood flow patterns and local hemodynamic parameters have been widely associated with the remodeling of vascular grafts. We use time-of-flight MRI to construct 3-dimensional computational models (**Figure 7F**). Hemodynamic parameters, including velocity, viscosity, wall shear, and wall pressure, were examined based on time-of-flight angiography (**Figure 7G**, Supplemental Figure 21). Disturbed blood flow with a low velocity was observed in the PCL group. Although both the PCL-TM group and PCL-GalS group displayed a higher flow rate than the PCL group, disturbed blood flow was evident at locations near the proximal anastomic site. In contrast, the PCL-TG group exhibited a laminar flow profile, particularly a high flow speed. Viscosity, as the main determinant of wall shear stress (WSS), has been demonstrated to be a powerful predictor of thrombus formation. The PCL-TG group had a lower and more homogeneous viscosity than the other groups. Another critical hemodynamic variable that triggers vascular remodeling post-implantation is WSS. Vascular graft areas with low or oscillating WSS are most prone to the development of atherosclerotic plaques. Interestingly, PCL-TG grafts showed a higher WSS than the other groups, suggesting that antithrombogenic surface modification promotes the desired hemodynamic adaptation.

ANTITHROMBOGENIC SURFACE MODIFICATION ENHANCES ENDOTHELIALIZATION AND REDUCES INTIMAL HYPERPLASIA IN PIGS. Hematoxylin and eosin staining was first performed to evaluate the vascular regeneration and remodeling in pigs. Serious intimal hyperplasia was identified in the PCL-TM vascular grafts, in contrast to the beneficial tissue regeneration in the PCL-TG group, as evidenced by a layer of neotissue with a well-defined structure (**Figure 8A**, Supplemental Figure 22). Quantitative analysis further confirmed that the lumen area of the PCL-TM group was significantly lower than those of other groups (**Figure 8B**). Endothelialization was further demonstrated by immunofluorescence

FIGURE 6 Continued

(A) Experimental schedule for the evaluation of vascular regeneration in functionalized vascular grafts. **(B)** H&E staining images showing the regeneration of neotissue in vascular grafts at 3 months. Scale bars = 500 μm **(top)**, 100 μm **(bottom)** (n = 6). **(C)** Endothelium regeneration was confirmed by eNOS **(red)** and CD144 **(green)** co-immunofluorescence staining of the cross-section of explanted vascular grafts at 3 months postimplantation. Scale bar = 100 μm. The number of CD144^{+} eNOS^{+} cells was further quantified (n = 6). **(D)** Cross-sections of vascular grafts explanted at 3 months were stained by MYH11 **(red)** and CNN1 **(green)**. Scale bar = 100 μm. The number of CNN1^{+} MYH11^{+} cells within the neotissue was further quantified (n = 6). **(E)** The physiological functions of the vascular grafts explanted at 3 months were assessed by wire myography. Drugs were added where indicated by symbol. Responses of the explanted grafts to KCl, adrenaline, and acetylcholine were analyzed (n = 3). Statistical significance was assessed by 1-way analysis of variance followed by Tukey's post hoc analysis. Data are expressed as mean ± SEM. *P < 0.05, **P < 0.01, and ***P < 0.001. Abbreviations as in **Figures 1 and 2**.

FIGURE 7 Antithrombogenic Surface Modification Enhances Patency of Vascular Grafts in a Pig Model

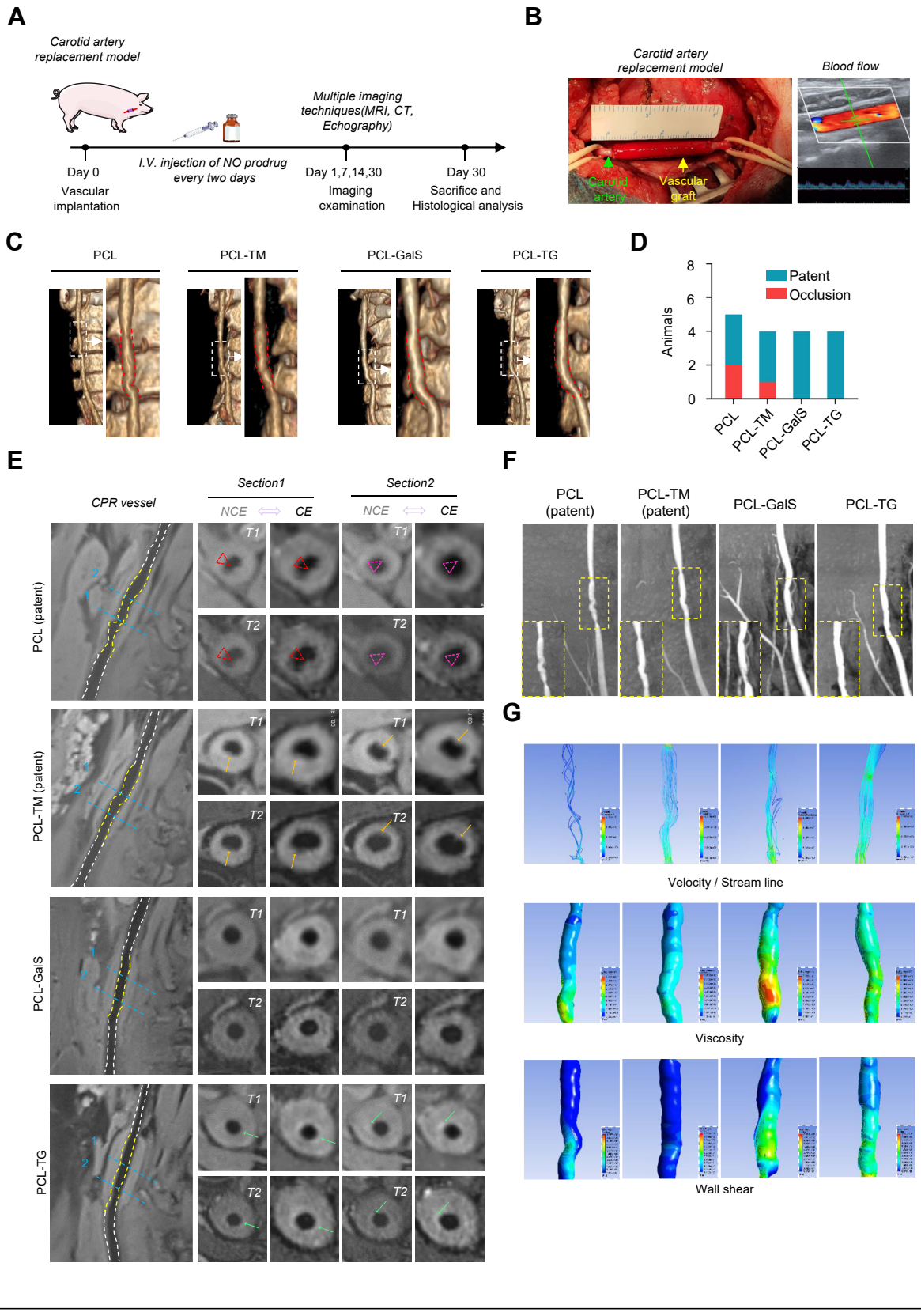

Continued on the next page

staining with CD31 antibody (**Figure 8C**, Supplemental Figure 23). Similarly, TM and NO cooperatively enhanced endothelialization with highest luminal coverage of $CD31^+$ cells obtained in the PCL-TG group (**Figure 8D**). Interestingly, the expression of KLF2 and its downstream genes (eNOS and TM) in ECs was also upregulated in the PCL-TG vascular grafts compared with other 3 groups due to the improved hemodynamics that is crucial for endothelial homeostasis via regulating endothelial function (**Figure 8D**).

Vascular smooth muscle regeneration was first assessed by α-SMA staining (**Figure 8E**, Supplemental Figure 24). The area of $\alpha\text{-SMA}^+$ cells was markedly higher in the PCL-TM group than in the other 3 groups, indicating intimal hyperplasia (**Figure 8F**). The regeneration of functional smooth muscle was further investigated by double immunofluorescence staining of α-SMA and the more specific markers of SMCs (MYH11 and CNN1). A well-organized layer of double-positive SMCs was observed in the PCL-TG vascular graft in contrast to other groups, especially the PCL-TM and PCL groups (**Figure 8E**). Quantitation of $\alpha\text{-SMA}^+$ $MYH11^+$ and $\alpha\text{-SMA}^+$ $CNN1^+$ cells further confirmed enhanced regeneration of contractile smooth muscle in the PCL-TG group (**Figure 8F**). ECM secretion of regenerated neotissue was also evaluated by Masson's trichrome staining. The results revealed that more muscle fibers formed in the PCL-TG group than that in other 3 groups (**Figure 8G**).

DISCUSSION

Thrombosis is a complex process that involves protein and cell adsorption, thrombin formation, and platelet activation and aggregation; therefore, surface modifications targeting only one aspect of thrombosis pathogenesis are unable to provide sufficient antithrombogenic efficacy.[29] The vascular endothelium is an ideal antithrombogenic surface that is pivotal for maintaining the long-term patency of native blood vessels.[14] Mimicking the functions of the endothelium on the graft surface is the most direct and effective approach to reduce thrombogenicity and thus improve the patency of vascular grafts. In this regard, recent attention has been given to engineering endothelium-mimetic surfaces/interfaces on artificial blood vessels. However, the regenerated endothelium is always incompetent and exhibits poorly formed cell junctions and reduced expression of antithrombotic molecules and NO production,[15] which often leads to late graft thrombosis.

Our results first demonstrated that endothelial dysfunction was common in the atherosclerotic lesions of patients undergoing carotid endarterectomy and was mainly attributed to reduced expression of TM and eNOS.

NO generated by eNOS is an important signaling molecule that regulates multiple physiological processes, including the activation and adhesion of leukocytes, platelet aggregation, thrombus formation, and endothelial integrity.[30,31] Clinical studies have shown that impairment of NO production may contribute to the development of atherothrombotic syndromes.[32,33] It has been reported that endothelial NO production is closely related to 5-year graft patency in patients receiving coronary artery bypass grafting.[34] Several studies have proven that low levels of NO produced by saphenous veins compared with that produced by arterial conduits may contribute to early graft failure.[35,36]

TM, a thrombin receptor expressed on ECs, is involved in activation of the anticoagulant protein C pathway during blood coagulation.[37] The risk of arterial thrombosis is increased approximately 5 times in patients with a mutation in the promoter region of the TM gene.[38] Clinical observations suggest that TM-mediated activation of protein C may be physiologically important in vessels with low flow

FIGURE 7 Continued

(A) Experimental schedule for the evaluation of the vascular graft in a pig model. **(B)** Implantation of the vascular graft to replace a segment of porcine carotid artery via interrupted anastomosis. The graft patency was detected by color Doppler ultrasonography after surgery. **(C)** Representative computed tomography angiographic images of patent vascular grafts. The implanted vascular grafts are indicated by **red dotted lines**. **(D)** The patency rate of vascular grafts at 1 month (n = 4 or 5). **(E)** Magnetic resonance imaging (MRI) of patent vascular grafts. The sagittal images **(left)** were scanned by 3-T MRI using curved planar reconstruction (CPR). The reconstruction line was traced along the course of the carotid artery. **Yellow dotted lines** indicate the lumen of implanted vascular grafts. T1 and T2 maps of the vascular grafts in the cross-section at the specified location (**blue dotted line** in CPR) are shown on the **right**, respectively. Contrast-enhanced (CE) images were obtained after a delay of 15 minutes following intravenous administration of contrast agent. Vascular remodeling was revealed through comparing the contrast enhanced images with non–contrast-enhanced (NCE) images in T1 and T2 phases. **Red arrowheads** indicate the mural thrombus. **Yellow arrows** indicate hyperplastic intima in the vascular grafts, while **green arrows** indicate the neotissue within the graft wall. **(F)** Time-of-flight MR angiography of vascular grafts at 1 month. **(G)** Hemodynamic reconstruction of vascular grafts. Velocity, viscosity and wall shear were analyzed based on the time-of-flight MR angiography. I.V. = intravenous; abbreviations as in **Figures 1 and 2**.

FIGURE 8 Antithrombogenic Surface Modification Promotes Endothelialization and Reduces Intimal Hyperplasia of Vascular Grafts in a Pig Model

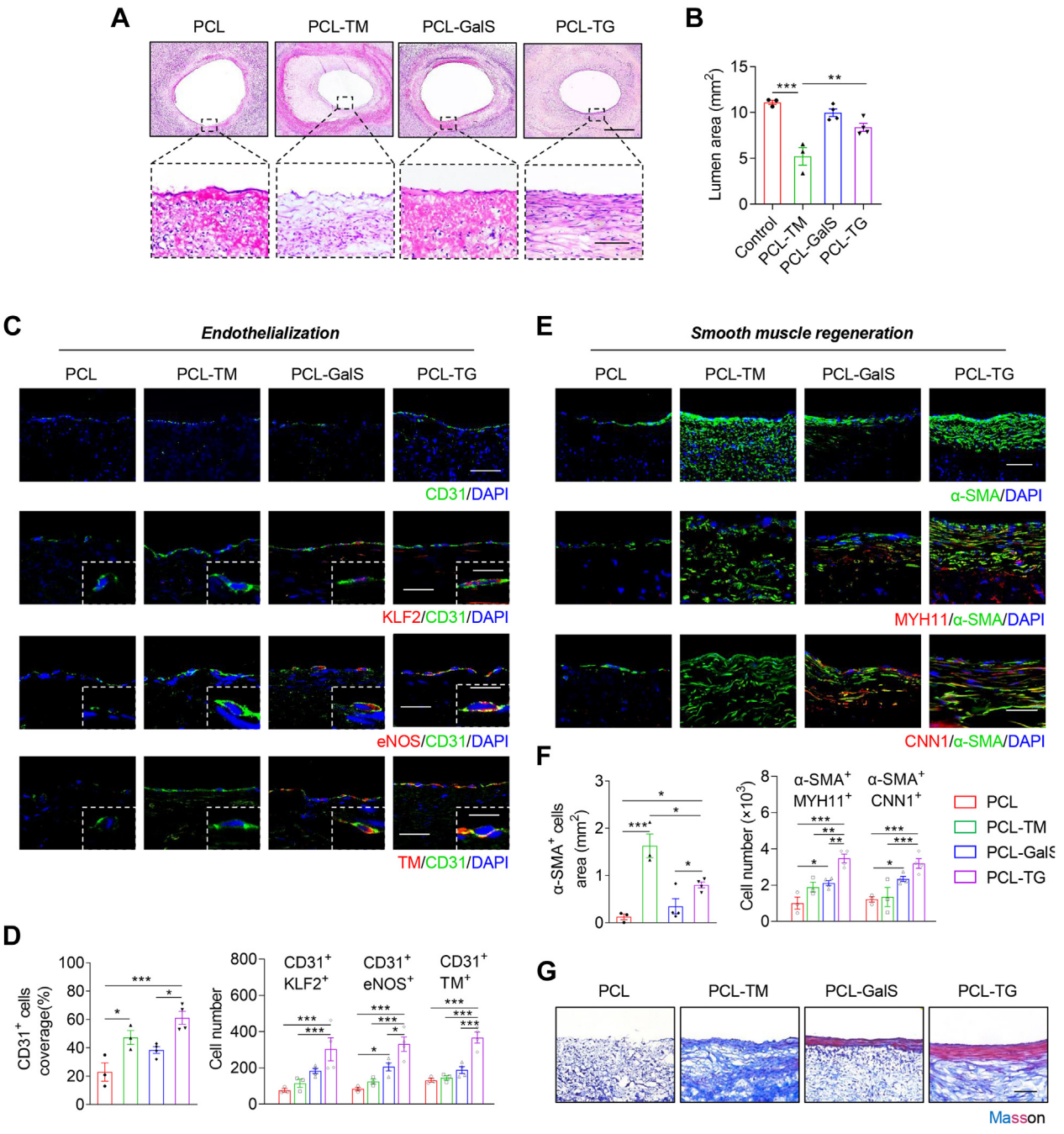

(A) Representative H&E staining images showing the lumen area of vascular grafts explanted at 1 month. Scale bars = 2 mm **(top)**, 200 μm **(bottom)**. **(B)** Quantification of the lumen area based on H&E staining. **(C)** Immunofluorescence staining of cross-sections by CD31. Scale bar = 100 μm. Endothelialization was further confirmed by immunofluorescence staining for CD31 **(green)** and KLF2 **(red)**, eNOS **(red)**, and thrombomodulin **(red)**, respectively. Nuclei were stained with DAPI **(blue)**. Scale bars = 10 μm. **(D)** The regeneration of endothelium was quantified by determining the coverage of $CD31^+$ cells on the luminal surface at different sites (suture, quarter, and middle). The number of $CD31^+$ $KLF2^+$, $CD31^+$ $eNOS^+$, and $CD31^+$ TM^+ cells was further quantified. **(E)** Immunofluorescence staining of cross-sections by α-SMA **(green)**. Scale bar = 100 μm. Smooth muscle regeneration was further analyzed by immunofluorescence staining for α-SMA **(green)** and MYH11 **(red)** and CNN1 **(red)**, respectively. Nuclei were stained with DAPI **(blue)**. Scale bar = 20 μm. **(F)** The area of $α\text{-SMA}^+$ cells as well as the number of $α\text{-SMA}^+$ $MYH11^+$ and $α\text{-SMA}^+$ $CNN1^+$ cells were quantified. **(G)** The secretion of collagen within the graft wall was analyzed by Masson staining. Scale bar = 100 μm. Statistical significance was assessed by 1-way or 2-way analysis of variance followed by Tukey's post hoc analysis. Data are expressed as mean ± SEM. PCL group (n = 3); PCL-TM group (n = 3); PCL-GalS group (n = 4); PCL-TG group (n = 4). $*P < 0.05$, $**P < 0.01$, and $***P < 0.001$. Abbreviations as in Figures 1 and 2.

rates.[39] A comparative study showed that the damage to vein grafts during harvest and storage results in a marked decrease in the ability to activate protein C, which contributes to early graft thrombosis.[40]

In this regard, supplementation of NO and TM to vascular grafts could recapitulate the antithrombotic function of the native endothelium in the early stage and promote the regeneration of endothelium afterward to guarantee the long-term patency of vascular grafts. In detail, a recombinant TM fragment and engineered galactosidase, a bump-and-hole–modified enzyme for a NO prodrug,[16] were co-immobilized onto vascular grafts under the catalysis of eSrtA in the present study. We found that TM and NO can synergistically inhibit thrombin activation and platelet adhesion and aggregation in both in vitro and in vivo assays. The patency of dual-modified (PCL-TG) vascular grafts was markedly improved in a clinically relevant porcine model, whereas mural thrombus and intimal hyperplasia caused occlusion of PCL and PCL-TM grafts. Furthermore, compared with TM or NO alone, TM and NO exerted antithrombogenic effects via distinct mechanisms, leading to cooperative effects. TM forms a high-affinity complex with thrombin, thus inhibiting the interaction of thrombin with procoagulant substrates. On the other hand, NO inhibits platelet adhesion, aggregation, and the formation of leukocyte-platelet aggregates mainly via the NO/cGMP signaling pathway.[41] Collectively, these results suggest that the combination of TM and NO inhibits multiple aspects of thrombosis.

In addition to the anticoagulation function, TM has also been accepted as a key angiogenic factor, and proangiogenic functions of TM are preserved in the C loop of the fifth epidermal growth factor-like domain.[42,43] Recent studies have further demonstrated that TM plays a vital role in maintaining the vascular integrity and quiescence of vascular ECs.[44] NO is also a key factor involved in neovascularization.[45,46] During the process of angiogenesis, NO not only induces endothelial migration and proliferation, but also modulates the secretion of other angiogenic factors.[47] As a result, the combination of TM and NO demonstrated a synergistic effect on enhancing endothelialization of vascular grafts, as confirmed in both rat and pig models.

While TM is an EC membrane-bound anticoagulant protein expressed in normal arteries, SMCs also express large amounts of TM that influences SMC behavior and induces neointima formation after vascular injury.[48] The TM expression in atherosclerotic lesions may be associated with promotion of atherosclerosis through its mitogenic activity in SMCs.[49] In this study, severe intimal hyperplasia was observed in the PCL-TM grafts because the recombinant TM fragment (epidermal growth factor-like domains 4-6) used in this study preserves the function related to mitogenic activity.[37] In contrast, NO secreted by native endothelium is an important contributor to the quiescence of SMCs; it effectively inhibits SMC proliferation after vascular injury by both cGMP-dependent pathway and NO-induced post-translational modifications.[50] Finally, the combination of TM and NO promoted the regeneration of functional smooth muscle and inhibited intimal hyperplasia and the subsequent restenosis.

STUDY LIMITATIONS. First, only a short period of observation was performed in large animal models. A long-term follow-up is needed in the future to further reveal the clinical potential of the vascular grafts. Second, animal studies were conducted by using healthy animals, which is inconsistent with the patients requiring bypass surgery in clinical setting. It is known that patients experience chronic diseases exhibit a diminished healing regeneration capacity. For example, the endothelial healing rate in the vascular graft could be slow in diabetic patients due to the dysfunctional migration and proliferation of endothelial cells in neighboring blood vessels. Third, although drugs can be delivered via central venous catheters for several weeks after bypass surgery, it is still likely to cause damages or undesirable side effects due to the multiple drug administration after the surgery. For this reason, delivery modality needs to be further optimized to develop safe (noninvasive) strategies that are more appropriate for clinical applications. Last, whether better outcomes can be achieved by modulating the dose of NO at different periods after graft implantation remains to be addressed in a larger scaled study.

CONCLUSIONS

In summary, we found that eNOS and TM are 2 important factors for the antithrombogenic function of the native endothelium and that deficiency of these proteins contributes to the development of thrombotic lesions in patients with atherosclerosis. In addition, 2 bioactive molecules, TM and GalS, which could catalyze the release of NO from the prodrug, were successfully immobilized on the surface of vascular grafts by an eSrtA-mediated ligation protocol. In vitro and in vivo assays both demonstrated that TM and NO exerted a synergistic effect to inhibit

thrombosis. As a result, patency and hemodynamic performance were improved in a clinically relevant porcine model. Interestingly, the antithrombogenic surface also promoted endothelialization while reducing adverse intimal hyperplasia through the cooperation between TM and NO.

FUNDING SUPPORT AND AUTHOR DISCLOSURES

This study is supported by the National Natural Science Foundation of China (Nos. 81925021, 82102223, U21A20391, 21977055, and 81901728) and National Key R&D Program of China (2018YFE0200503). The authors have reported that they have no relationships relevant to the contents of this paper to disclose.

ADDRESS FOR CORRESPONDENCE: Dr Qiang Zhao, College of Life Sciences, Nankai University, Nankai District, Tianjin 300071, China. E-mail: qiangzhao@nankai.edu.cn; OR Dr Jiansong Cheng, College of Pharmacy, Nankai University, Tianjin 300353, China. E-mail: jiansongcheng@nankai.edu.cn.

PERSPECTIVES

COMPETENCY IN MEDICAL KNOWLEDGE: TM and eNOS were key factors for the antithrombogenic function of the endothelium in human arteries. Surface modification via immobilization of recombinant TM and an engineered galactosidase cooperatively enhanced the antithrombogenicity and patency of the vascular grafts.

TRANSLATIONAL OUTLOOK: Additional preclinical studies are required to determine whether biomimetic surface modification is beneficial in graft patency and vascular homeostasis after long-term implantation. Assessments on the biosafety of the vascular grafts in human are also needed as a prelude to clinical trials.

REFERENCES

1. Roth GA, Mensah GA, Johnson CO, et al. Global Burden of Cardiovascular Diseases and Risk Factors, 1990-2019: update from the GBD 2019 study. *J Am Coll Cardiol*. 2020;76:2982–3021.

2. Weintraub WS, Grau-Sepulveda MV, Weiss JM, et al. Comparative effectiveness of revascularization strategies. *N Engl J Med*. 2012;366:1467–1476.

3. Li S, Sengupta D, Chien S. Vascular tissue engineering: from in vitro to in situ. *Wiley Interdiscip Rev Syst Biol Med*. 2014;6:61–76.

4. Dahl SL, Kypson AP, Lawson JH, et al. Readily available tissue-engineered vascular grafts. *Sci Transl Med*. 2011;3:68ra9.

5. Syedain ZH, Graham ML, Dunn TB, et al. A completely biological "off-the-shelf" arteriovenous graft that recellularizes in baboons. *Sci Transl Med*. 2017;9:eaan4209.

6. Pektok E, Nottelet B, Tille JC, et al. Degradation and healing characteristics of small-diameter poly(epsilon-caprolactone) vascular grafts in the rat systemic arterial circulation. *Circulation*. 2008;118:2563–2570.

7. Wu W, Allen RA, Wang Y. Fast-degrading elastomer enables rapid remodeling of a cell-free synthetic graft into a neoartery. *Nat Med*. 2012;18:1148–1153.

8. Kirkton RD, Santiago-Maysonet M, Lawson JH, et al. Bioengineered human acellular vessels recellularize and evolve into living blood vessels after human implantation. *Sci Transl Med*. 2019;11:eaau6934.

9. Drews JD, Pepper VK, Best CA, et al. Spontaneous reversal of stenosis in tissue-engineered vascular grafts. *Sci Transl Med*. 2020;12:eaau6934.

10. Lawson JH, Glickman MH, Ilzecki M, et al. Bioengineered human acellular vessels for dialysis access in patients with end-stage renal disease: two phase 2 single-arm trials. *Lancet*. 2016;387:2026–2034.

11. Dimitrievska S, Wang J, Lin T, et al. Glycocalyx-like hydrogel coatings for small diameter vascular grafts. *Adv Funct Mater*. 2020;30:1908963.

12. Hoshi RA, Van Lith R, Jen MC, Allen JB, Lapidos KA, Ameer G. The blood and vascular cell compatibility of heparin-modified ePTFE vascular grafts. *Biomaterials*. 2013;34:30–41.

13. Durán-Rey D, Crisóstomo V, Sánchez-Margallo JA, Sánchez-Margallo FM. Systematic review of tissue-engineered vascular grafts. *Front Bioeng Biotechnol*. 2021;9:771400.

14. Seifu DG, Purnama A, Mequanint K, Mantovani D. Small-diameter vascular tissue engineering. *Nat Rev Cardiol*. 2013;10:410–421.

15. Otsuka F, Finn AV, Yazdani SK, Nakano M, Kolodgie FD, Virmani R. The importance of the endothelium in atherothrombosis and coronary stenting. *Nat Rev Cardiol*. 2012;9:439–453.

16. Hou J, Pan Y, Zhu D, et al. Targeted delivery of nitric oxide via a 'bump-and-hole'-based enzyme-prodrug pair. *Nat Chem Biol*. 2019;15:151–160.

17. Ham HO, Qu Z, Haller CA, et al. In situ regeneration of bioactive coatings enabled by an evolved Staphylococcus aureus sortase A. *Nat Commun*. 2016;7:11140.

18. Huang J, Pu Y, Zhang H, et al. KLF2 mediates the suppressive effect of laminar flow on vascular calcification by inhibiting endothelial BMP/SMAD1/5 signaling. *Circ Res*. 2021;129:e87–e100.

19. Jiang R, Weingart J, Zhang H, Ma Y, Sun XL. End-point immobilization of recombinant thrombomodulin via sortase-mediated ligation. *Bioconjug Chem*. 2012;23:643–649.

20. Zhang J, Wang J, Wei Y, et al. ECM-mimetic heparin glycosamioglycan-functionalized surface favors constructing functional vascular smooth muscle tissue in vitro. *Colloids Surf B Biointerfaces*. 2016;146:280–288.

21. Wei Y, Wu Y, Zhao R, et al. MSC-derived sEVs enhance patency and inhibit calcification of synthetic vascular grafts by immunomodulation in a rat model of hyperlipidemia. *Biomaterials*. 2019;204:13–24.

22. Kim AY, Walinsky PL, Kolodgie FD, et al. Early loss of thrombomodulin expression impairs vein graft thromboresistance: implications for vein graft failure. *Circ Res*. 2002;90:205–212.

23. Adam PC, Marisa KL, Stephen GW. Chemokine signalling: pivoting around multiple phosphoinositide 3-kinases. *Immunology*. 2002;105:125–136.

24. Cai H, Ken J, Michael DS. MAP kinases and cell migration. *J Cell Sci*. 2004;117:4619–4628.

25. Zheng J, Wen YX, Austin JL, Chen DB. Exogenous nitric oxide stimulates cell proliferation via activation of a mitogen-activated protein kinase pathway in ovine fetoplacental artery endothelial cells. *Biol Reprod*. 2006;74:375–382.

26. Wang KC, Li YH, Shi GY, et al. Membrane-bound thrombomodulin regulates macrophage inflammation in abdominal aortic aneurysm. *Arterioscler Thromb Vasc Biol*. 2015;35:2412–2422.

27. Huang TC, Wu HL, Chen SH, Wang YT, Wu CC. Thrombomodulin facilitates peripheral nerve regeneration through regulating M1/M2 switching. *J Neuroinflammation*. 2020;17:240.

28. Zhu D, Hou J, Qian M, et al. Nitrate-functionalized patch confers cardioprotection and improves heart repair after myocardial infarction via

local nitric oxide delivery. *Nat Commun*. 2021;12:4501.

29. Jordan SW, Chaikof EL. Novel thrombor-esistant materials. *J Vasc Surg*. 2007;45(Suppl A):A104–A115.

30. Ramesh S, Morrell CN, Tarango C, et al. Antiphospholipid antibodies promote leukocyte-endothelial cell adhesion and thrombosis in mice by antagonizing eNOS via β2GPI and apoER2. *J Clin Invest*. 2011;121:120–131.

31. de Mel A, Murad F, Seifalian AM. Nitric oxide: a guardian for vascular grafts? *Chem Rev*. 2011;111:5742–5767.

32. Freedman JE, Ting B, Hankin B, Loscalzo J, Keaney JF Jr, Vita JA. Impaired platelet production of nitric oxide predicts presence of acute coronary syndromes. *Circulation*. 1998;98:1481–1486.

33. Loscalzo J. Nitric oxide insufficiency, platelet activation, and arterial thrombosis. *Circ Res*. 2001;88:756–762.

34. Suvorava T, Dao VT, Bas M, Kojda G. Nitric oxide and the CABG patient. *Curr Opin Pharmacol*. 2012;12:195–202.

35. Lüscher TF, Diederich D, Siebenmann R, et al. Difference between endothelium-dependent relaxation in arterial and in venous coronary bypass grafts. *N Engl J Med*. 1988;319:462–467.

36. Liu ZG, Ge ZD, He GW. Difference in endothelium-derived hyperpolarizing factor-mediated hyperpolarization and nitric oxide release between human internal mammary artery and saphenous vein. *Circulation*. 2000;102:III296–III301.

37. Loghmani H, Conway EM. Exploring traditional and nontraditional roles for thrombomodulin. *Blood*. 2018;132:148–158.

38. Ireland H, Kunz G, Kyriakoulis K, Stubbs PJ, Lane DA. Thrombomodulin gene mutations associated with myocardial infarction. *Circulation*. 1997;96:15–18.

39. Bakoush O, Ohlin AK, Strandberg K, Kurkus J. Low plasma activated protein C-protein C inhibitor complex concentration is associated with vascular access failure in hemodialysis patients. *Nephron Clin Pract*. 2008;110:c151–c157.

40. Cook JM, Cook CD, Marlar R, Solis MM, Fink L, Eidt JF. Thrombomodulin activity on human saphenous vein grafts prepared for coronary artery bypass. *J Vasc Surg*. 1991;14:147–151.

41. Isenberg JS, Romeo MJ, Yu C, et al. Thrombospondin-1 stimulates platelet aggregation by blocking the antithrombotic activity of nitric oxide/cGMP signaling. *Blood*. 2008;111:613–623.

42. Wang X, Pan B, Honda G, et al. Cytoprotective and pro-angiogenic functions of thrombomodulin are preserved in the C loop of the fifth epidermal growth factor-like domain. *Haematologica*. 2018;103:1730–1740.

43. Shi CS, Shi GY, Chang YS, et al. Evidence of human thrombomodulin domain as a novel angiogenic factor. *Circulation*. 2005;111:1627–1636.

44. Giri H, Panicker SR, Cai X, Biswas I, Weiler H, Rezaie AR. Thrombomodulin is essential for maintaining quiescence in vascular endothelial cells. *Proc Natl Acad Sci U S A*. 2021;118:e2022248118.

45. Duda DG, Fukumura D, Jain RK. Role of eNOS in neovascularization: NO for endothelial progenitor cells. *Trends Mol Med*. 2004;10:143–145.

46. Kashiwagi S, Izumi Y, Gohongi T, et al. NO mediates mural cell recruitment and vessel morphogenesis in murine melanomas and tissue-engineered blood vessels. *J Clin Invest*. 2005;115:1816–1827.

47. Namba T, Koike H, Murakami K, et al. Angiogenesis induced by endothelial nitric oxide synthase gene through vascular endothelial growth factor expression in a rat hindlimb ischemia model. *Circulation*. 2003;108:2250–2257.

48. Wang KC, Chen PS, Chao TH, et al. The role of vascular smooth muscle cell membrane-bound thrombomodulin in neointima formation. *Atherosclerosis*. 2019;287:54–63.

49. Tohda G, Oida K, Okada Y, et al. Expression of thrombomodulin in atherosclerotic lesions and mitogenic activity of recombinant thrombomodulin in vascular smooth muscle cells. *Arterioscler Thromb Vasc Biol*. 1998;18:1861–1869.

50. Napoli C, Paolisso G, Casamassimi A, et al. Effects of nitric oxide on cell proliferation: novel insights. *J Am Coll Cardiol*. 2013;62:89–95.

KEY WORDS antithrombogenic surface modification, endothelialization, nitric oxide, thrombomodulin, vascular grafts

APPENDIX For an expanded Methods section and supplemental tables and figures, please see the online version of this paper.